An Enhanced Pathfinder Algorithm for Optimal Integration of Solar Photovoltaics and Rapid Charging Stations in Low-Voltage Radial Feeders

Thandava Krishna Sai Pandraju[a], Varaprasad Janamala[b*]

aDepartment of Electrical and Electronics Engineering, Dhanekula Institute of Engineering and Technology, Vijayawada - 521139, Andhra Pradesh, India.
bDepartment of Electrical and Electronics Engineering, School of Engineering and Technology, CHRIST (Deemed to be University), Bangalore-560074, Karnataka, India.

ARTICLE INFO

A B S T R A C T

Most low-voltage (LV) feeders have large distribution losses, poor voltage profiles, and inadequate voltage stability margins owing to their radial construction and high R/X ratio branches, and they may not be able to handle substantial solar photovoltaics (SPVs) and EV penetration. Thus, optimal integration of SPVs and rapid charging stations (RCSs) can solve this problem. This paper offers an extended pathfinder algorithm (EPFA) with guiding elements and three followers' life lifestyle procedures based on animal foraging, exploitation, and killing. First, the EV load penetration was used to evaluate the LV feeder performance. Subsequently, the required RCSs and SPVs were appropriately integrated to match the EV load penetration and optimise feeder performance. An Indian 85-bus real-time system was used for simulations. The losses and GHG emissions increased by 150% and 80%, respectively, without the SPVs and RCS for zero-to-full EV load penetration. RCSs allocation alone reduced the losses by 40.1%, whereas simultaneous SPVs and RCSs allocation reduced the losses by 66%. However, the GHG emissions decreased by 13.7% and 54.33%, respectively. This study shows that SPVs and RCS can enhance the LV feeder performance both technically and environmentally. In contrast, EPFA outperformed the other algorithms in terms of the global solution and convergence time.

1. Introduction

Global warming has emerged as one of the primary challenges of the twenty-first century. With the goal of achieving sustainable development, the incorporation of renewable energy (RE) has emerged as a promising solution, particularly in the context of SDG 7: affordable and clean energy. By

*Corresponding Author Email: varaprasad.janamala@christuniversity.in

analysing Ember's Yearly Electricity Data [1] for 2021 and 2022, notable trends in global power generation became apparent. Hydroelectric power generation has witnessed a moderate increase of 1.94% in 2022, reaching a total of 4326.76 TWh. Wind power generation experienced a significant surge of 15.67%, surpassing the 2000 TWh mark and reaching 2139.23 TWh in 2022. Similarly, solar power generation exhibited a substantial growth of 23.96%, amounting to 1289.27 TWh in 2022. Solar energy, in particular, has gained significant momentum across various countries owing to its ease of installation, low maintenance requirements, and clean and noiseless operation. Furthermore, other renewable energy sources also witnessed a modest increase of 2.44%, reaching a total generation of 777.31 TWh in 2022. These findings underscore the escalating prominence of RE as a viable and sustainable energy option, heralding a promising future for the global energy landscape.

Electric vehicles (EVs) are crucial for decarbonizing road transport, accounting for almost 15% of global energy-related emissions, and EV adoption has increased dramatically in recent years, along with improvements in range, model diversity, and performance, according to the International Energy Agency (IEA) [2]. In particular, passenger electric automobiles have grown in popularity, with forecasts predicting 18% of new car sales by 2023. This amazing rise signals a transition toward a more sustainable and environmentally conscious car sector.

However, despite the numerous environmental and flexibility benefits associated with RE and EVs, it is crucial to address various technical challenges, such as stability (including transient, dynamic, and small-signal stability), energy balance, security, reliability, and power quality. These concerns arise because of the intermittent nature of RE sources and stochastic behaviour of EVs. In the literature, considerable attention has been paid to the optimal integration of RE-based distribution generation (OADG), particularly solar photovoltics (SPV) and wind turbines (WT) in electrical distribution networks (EDNs), specifically those with radial structures characterised by high R/X ratios and low voltage. This integration aims to minimise the distribution losses, improve the voltage profiles, and enhance the voltage stability margins as highlighted by H. A. et al. [3].

While the OADG problem has been successfully addressed using various analytical techniques discussed by Ehsan et al. [4], meta-heuristic approaches (MHA) have gained popularity among researchers owing to their simplicity, derivative-free nature, and applicability to diverse optimisation problems, as comprehensively reviewed by Tolba et al. [5]. Several MHAs have been employed to address the OADG problem and optimise the placement and sizing of DG units. One approach by Reddy et al. [6] involves the use of a whale optimisation algorithm (WOA) inspired by humpback whale hunting behaviour to identify the optimal size of different types of DG units (i.e. SPV, WT, wind, and capacitors). Similarly, Reddy et al. [7] also proposed the ant lion optimisation (ALO) algorithm, which mimics the hunting behaviour of ant lions, to optimise the sizing of DG units along with the index vector (IV) approach to determine the most suitable locations for SPV, WT, and capacitors. Suresh et al [8] are introduced the dragonfly algorithm (DA) was utilised in another study to calculate the appropriate sizes of PV and WT units, considering various factors, such as voltage profile, regulation, stability, power losses, and economic benefits. Reddy et al. [9] employed the index vector (IV) approach has also been used to optimise the placement of SPV and WT units. Furthermore, the flower pollination algorithm (FPA) determines the ideal size of DG units to reduce power losses and improve the voltage profiles. ChithraDevi et al. [10] was employed the stud krill herd algorithm (SKHA) to solve the optimal placement and sizing of single and multiple SPV based DGs in radial distribution networks (RDNs) with the primary objective of reducing line losses for different loading conditions. The location and size of SPV and WT-based DGs were determined using loss sensitivity factors (LSFs) and ALO to reduce real power losses and improve the voltage profile by Ali et al.[11]. Hemeida et al. [12] utilized the Manta Ray Foraging Optimization (MRFO) algorithm to minimize power losses by optimizing the sizing and allocation of SPV systems in radial EDNs. Prabha et al. [13] employed loss sensitivity factors (LSFs) to determine the optimal placement of SPV-based DGs. Subsequently, the invasive weed optimization (IWO) algorithm was used to determine the appropriate DG sizes. The objective was to reduce the real power loss, operating costs, and improve the voltage stability under various load conditions. Hemeida et al. [14] applied several optimization algorithms, including grey wolf optimization (GWO), MRFO, satin bower bird optimization (SBO), and water optimization algorithm (WOA) for solving the SPV allocation problem. They considered the load uncertainty and used Monte Carlo simulation to optimize the allocation strategy.

Ali et al. [15] focused on enhancing the reliability and efficiency of uncertain EDNs by solving the SPV and WT-based optimal allocation of distributed generators (OADG) problem. They utilized an improved wild-horse optimization (IWHO) algorithm for this purpose. Janamala et al. [16] focused on Archimedes optimization algorithm (AOA) to optimize the allocation of SPV-based DGs in Indian agricultural feeders. The objective was to achieve a balance between the technical and environmental factors. Selim et al. [17] developed an improved harris hawks optimization (IHHO) algorithm to address the allocation problem of SPV and WT-based DGs. This study considered multiple objectives, including loss reduction, voltage deviation minimization, and voltage stability enhancement. Janamala et al. [18] were applied the future search algorithm (FSA) to optimize SPV and WT-based DGs allocation, with a focus on loss reduction, voltage profile improvement, and voltage stability enhancement. Bhadoriya et al. [19] was used transient search optimization (TSO) to address similar objectives of SPV and WT-based DGs allocation for loss reduction and voltage profile improvement. Shahzad et al. [20] was applied the strawberry plant propagation algorithm (SPPA) to optimize the allocation of SPV and WT-based DGs, aiming to improve loss reduction, voltage profiles, and voltage stability. Akbar et al. [21] was employed an algorithm known as improved grey wolf optimization with particle swarm optimization (I-GWOPSO) to optimize the allocation of SPV and WT-based DGs, targeting loss reduction, voltage profile improvement, and voltage stability enhancement.

Researchers have also focused on the optimal allocation of charging stations (OACS) for EVs and their impact on electrical distribution feeders, as reviewed by Das et al. [22]. Zeb et al. [23] is employed particle swarm optimization (PSO) to optimally integrate three types of EV charging stations (i.e. levels 1, 2, and 3) in EDNs considering techno-economic benefits and PV uncertainties. Khan et al. [24] optimized grid-to-vehicle (G2V) and vehicle-to-grid (V2G) power flows at fast EV charging stations integrated with PVs by aiming power quality (PQ) improvement. Dai et al. [25] was proposed a multi-agent PSO (MAPSO) for optimally sizing the SPV /BESS/ EV-CSs components, considering overall cost optimisation as the major objective. Injeti et al. [26] were adapted the PSO and butterfly optimisation algorithm (BOA) to solve the optimal integration of SPV and WT based DGs in EDNs by considering different charging scenarios

for plug-in EVs. The optimisation methodology focuses on loss reduction and voltage profile improvements.

In light of the above reviewed works, this paper makes the following major contributions for handling the adverse effects of EV load penetration on LV feeders by optimal integration of RE-based DGs. Recently, the pathfinder algorithm (PFA) introduced by Yapici et al. [27] has received considerable attention for solving various complex optimization problems. However, its local optima trap and premature convergence were overcome in the enhanced pathfinder algorithm (EPFA) by incorporating guided and social influencing mechanisms in Tang et al. [28]. As per author's knowledge, integration of RCSs in RDNs along with SPVs and WTs is not much focused in literature. In additon, the EPFA was adapted for the first time to solve this problem.

Initially, the optimal integration of SPVs and WTs is addressed and the effectiveness of the EPFA is compared to that in the literature. Subsequently, the impact of EV load penetration on LV feeders was analysed using a voltage-dependent battery load model. The normalised voltage stability index (NVSI) was utilised to determine optimal locations for renewable charging stations (RCSs) integration. The real power loss, voltage stability and greenhouse gas (GHG) emissions provide a multi-objective function. Simulations were performed on an 85-bus urban Indian low-voltage feeder for the different scenarios.

The rest of the paper is organised as follows: Section 2 discusses the PV, WT, and EV load models mathematically. Section 3 presents the multi-objective function and limitations. Section 4 introduces the concept of PFA and its mathematical improvements. Section 5 discusses the simulation results of the EPFA and Section 6 emphasises the conclusion and future scope.

2. Modeling of Theoretical Concepts

In this section, mathematical modelling of DGs, BESS, and different types of loads is discussed for incorporating backward/forward sweep (BFS) load flow method by Eminoglu et al. [29].

2.1. Renewable Distribution Generation

According to power compensation, the DGs are categorised as Type-1 (real power generators such as SPV, fuel cells, and batteries), Type-2 (reactive power generators such as capacitors and

synchronous condensers), Type-3 (both real and reactive power generators such as WT), and Type-4 (real power generation and reactive power absorption such as micro turbines and synchronous generators) [3, 4]. By having a DG at a load point, its impact can be realised using Eqs. (1) and (2) as explained by Reddy et al. [6, 7].

$$P_{d,new(k)} = P_{d,base(k)} - P_{rdg(k)} \quad (1)$$

$$Q_{d,new(k)} = Q_{d,base(k)} - P_{rdg(k)} \times \tan(\phi_{rdg(k)}) \quad (2)$$

For an SPV-type DG, the power factor is considered to be 1, thus, the reactive power contribution becomes zero. WT-type DGs can be optimized between 0.3 and 1.

2.2. Network Load Profile

Specifically, EDNs associated with multiple types of consumers and their associated loads are highly dependent on voltage variations in the network. To accommodate changes in the voltage profile, this study was considered voltage-dependent load modelling. The following Eq. (3) and Eq. (4) were proposed for net real and reactive power loads considering different types of loads (i.e., residential, industrial, commercial and electric vehicles) using the voltage-dependent load modelling of Eminoglu et al. [29].

$$P_{d,new(k)} = P_{d,base(k)} \times \left\{ \begin{matrix} \lambda_r \left(\frac{|V_{(k)}|}{|V_{(r)}|}\right)^{\alpha_r} + \lambda_i \left(\frac{|V_{(k)}|}{|V_{(r)}|}\right)^{\alpha_i} + \\ \lambda_c \left(\frac{|V_{(k)}|}{|V_{(r)}|}\right)^{\alpha_c} + \lambda_{ev} \left(\frac{|V_{(k)}|}{|V_{(r)}|}\right)^{\alpha_{ev}} \end{matrix} \right\} \quad (3)$$

$$Q_{d,new(k)} = Q_{d,base(k)} \times \left\{ \begin{matrix} \lambda_r \left(\frac{|V_{(k)}|}{|V_{(r)}|}\right)^{\beta_r} + \lambda_i \left(\frac{|V_{(k)}|}{|V_{(r)}|}\right)^{\beta_i} + \\ \lambda_c \left(\frac{|V_{(k)}|}{|V_{(r)}|}\right)^{\beta_c} + \lambda_{ev} \left(\frac{|V_{(k)}|}{|V_{(r)}|}\right)^{\beta_{ev}} \end{matrix} \right\} \quad (4)$$

3. Problem Formulation

This section provides details of the proposed multi-objective function and with its design and operational constraints.

3.1. Multi-Objective Function

The objective function is aimed at reducing the total real power distribution loss, enhancing voltage stability and reducing GHG emissions from the main grid. Mathematically,

$$MOF = P_{loss(h)} + NVSI + GHG_{(h)} \quad (5)$$

$$P_{loss(h)} = \sum_{k=1}^{nbr} I_{k(h)}^2 r_{(k)} \quad (6)$$

$$NVSP = \max(NVSI_2, ..., NVSI_{nbus}) < 1 \quad (7)$$

Abdel-Akher et al. [30] developed a novel normalised voltage stability index (NVSI) defined in Eq. (8) to assess the stability of EDNs. Furthermore, the GHG emissions from the main grid owing conventional power plants can be assessed using Eq. (9) as described by Janamala et al. [31].

$$NVSP_p = 1 - \left[2(P_q r_k + Q_q x_k) - |V_{(p)}|^2 \right]^2 - \\ [4(P_q^2 + Q_q^2)(r_k^2 + x_k^2)], p = 2 : nbus \quad (8)$$

$$GHG_{(h)} = (CO_2 + NO_2 + SO_2) \times P_{d(s/s)} \quad (9)$$

3.2. Planning and Operational Constraints

The following bus voltage magnitudes, DG real and reactive power capacities, are the major constraints considered by Rani et al. [32].

$$|V|_{min} \leq V_{(k)} | \leq |V|_{max} \quad (10)$$

$$\sum_{k=1}^{ndg} P_{dg(k)} \leq \sum_{k=1}^{nbus} P_{d(k)} \quad (11)$$

$$\sum_{k=1}^{ndg} Q_{dg(k)} \leq \sum_{k=1}^{nbus} Q_{d(k)} \quad (12)$$

4. Solution Methodology

The concept of the pathfinder algorithm (PFA) and its hybrid approach for solving the optimal DG allocation along with the real power loss sensitivity index are explained in this section.

4.1. Basic Pathfinder Algorithm

Following social hierarchy, some animals migrate seasonally. In 2019, Yapici et al. [27] introduced the pathfinder algorithm (PFA), motivated by animal foraging, exploitation, and hunting. PFA's computational approach includes

leading a swarm for successful hunting and encouraging others to follow it. The planned PFA maintains best pathfinder position. Pathfinders know how to hunt and eat. The pathfinder and neighbours work together to investigate and exploit the objective in the search space. Controlling parameters prevent PFA local optima. PFA solves the optimization problems well. This section describes PFA's initialization, iteration, and halting of the mathematical model.

In an *n*-dimensional search space, a leader and pathfinder are an animal from a swarm equal to the number of search variables that determine the optimum hunting region for a prey. At the initialization stage of any heuristic search algorithm, the best fitness value is found among all the solutions from the original population. The initial population was generated using Eq. (13) Yapici et al. [27].

$$a_{i(0)}(k) = l_b + (u_b - l_b)*rand(1,d) \tag{13}$$

where $a_{i(0)}(k)$ is the position vector of animal-*i* at the start, *d* is the search space dimension, and l_b and u_b are the lower and upper variables in the optimization problem.

All other followers' actions with regard to changes in their position and time were modelled according to Eq. (14) Yapici et al. [27].

$$a_{i(k+1)} = a_{i(k)} \times x'+I_{ij} + G_a + V_v \tag{14}$$

where *k* denotes the passage of iteration, $a_{i(0)}$ and $a_{i(k)}$ denote the position vectors of individual animals *I* at their initial stages and iteration-*k*, respectively; *x'* denotes a unit vector with zero angle; I_{ij} denotes the interaction between two neighbours, *i* and *j*; G_a denotes the fitness that has been determined to be the best overall so far, or pathfinder fitness; and V_v denotes a vibration vector.

When this occurs, the position of the pathfinder is updated with the help of Eq. (15) Yapici et al. [27].

$$a_{p(k+1)} = a_{p(k)} + \Delta a_p + f_v \tag{15}$$

where pathfinder / animal a's initial and iteration-*k* positions are represented by the vectors; $a_{p(0)}$ and $a_{p(k)}$, respectively; Δa_p represents the pathfinder's position change, while f_v represents the fluctuation rate.

The following modifications are suggested for the collective movement of swimmers by altering Eq. (14) and (15) into Eq. (16) and (17) to resolve the optimization problem Yapici et al. [27].

$$a_i(k+1) = a_i(k) + \gamma.r_1.[a_j(k) - a_i(k)] \\ + \delta.r_2.[a_j(k) - a_i(k)] + V_v, i \geq 2 \tag{16}$$

$$a_p(k+1) = a_p(k) + \\ \gamma.r_3.[a_p(k) - a_p(k-1)] + f_v \tag{17}$$

$$V_v = (1 - \frac{k}{k_{max}}).u_1.D_{ij} \,\& V_f = u_2.e^{\left(\frac{-2k}{k_{max}}\right)} \tag{18}$$

$$D_{ij} = |a_i(k) - a_j(k)| \tag{19}$$

where γ is the interaction coefficient for defining the strength of interaction with a neighbour, δ is the attraction coefficient for setting the random distance for an individual with a group, preferably with a pathfinder, and k_{max} is the maximum number of iterations. r_1, r_2 and r_3 are uniformly distributed random numbers in the range [0, 1], and u_1 and u_2 are random vectors in the range [-1, 1] and have a range of [1, 2].

For example, V_v and V_f are generated at each iteration of the random walk in multiple dimensions for each animal in the group. However, to avoid the possibility of a local optima trap and premature convergence, improvements were proposed in both the pathfinder and follower stages in EPFA by Tang et al. [28].

In EPFA, the pathfinder is used as a guide to guide the agent that follows it to strengthen the link between them and increase algorithm mining. The modifications in the follower stage in the EPFA are the mutation mechanism, communication operator, and acceptance operator. Life systems allow three search space options for followers. (i) It can update its position across the search space and follow the direction of the leader. (ii) When searching, the algorithm follows the leader's general direction. (iii) As the leader's recommended action does not meet its requirements, he seeks a new approach. This stage enhances basic PFA algorithmic exploration. Furthermore, Tang et al. [28] illustrated the increased knowledge of swimming movements in relation to variations in γ, δ, u_1 and u_2.

4.2. Enhanced Pathfinder Algorithm

The pathfinder with the best target value is treated as a guide in each iteration and tries to share

information and experience with the followers. This can accelerate convergence. These modifications were mathematically described by Tang et al. [28].

$$a_{i(k)}(k+1) = a_{i(0)}(k) + \\ r_4\{a_{i(g)}(k) - w_p.mean[a_{i(0)}(k)]\} \quad (20)$$

where $a_{i(g)}(k)$ is the guide at iteration k, $w_p = round[1 + r_5(2-1)]$, r_4 and r_5 are the random numbers, $mean[a_{i(0)}(k)]$ is the mean of all followers in the same iteration.

In the follower phase, two operators were proposed to control the search direction. For a random number $r_6 > P = 0.8$, accept operator is used to update the position using Eq. (21). Otherwise, an exchange operator is added to update the followers using Eq. (22) and Eq. (23), where r_7, r_8, r_9 and r_{10} are random numbers between 0 and 1. The value of ρ determines the level of engagement with the leader or nearby individuals as developed by Tang et al. [28].

$$a_{i(k)}(k+1) = a_{i(0)}(k) + \\ 2(r_7 - 0.5)[a_{i(g)}(k) - a_{i(0)}(k)] \quad (21)$$

$$a_{i(k)}(k+1) = a_{i(0)}(k) + \rho.r_8.[a_{i(g)}(k) - \\ a_{i(0)}(k)] + \rho.r_9.[a_{j(0)}(k) - a_{i(0)}(k)] + \varepsilon, \varepsilon \geq 2 \quad (22)$$

$$\rho = \begin{cases} \frac{1}{2.r_{10}^{\sigma+1}} \rightarrow r_{10} \leq 0.5 \\ \left(\frac{1}{2(1-r_{10})}\right)^{\frac{1}{\sigma+1}} \rightarrow else \end{cases} \quad (23)$$

By gaining knowledge from and conversing with the leader and nearby folks, the person chooses their own search direction. The exploitation capability of the algorithm is enhanced by this procedure.

5. Simulation Results

The proposed EPFA methodology for the optimal allocation of RCSs and RESs was implemented on a real-time 85-bus LV urban feeder in Mysore city, Karnataka, India Janamala et al. [16]. The feeder has 84-branches, 85 buses, and a total composite load (i.e., 50% residential, 30% commercial and 20% industrial) of (2395.62 kW + j 1926.84 kVAr) at 11 kV. In the base case (i.e. without EV load penetration, $\lambda_{ev} = 0$), the feeder performance was determined using the load flow method proposed by Eminoglu et al. [29]. The composition of the residential, commercial and industrial loads at each

bus and in this work, are considered to be 0.5, 0.3 and 0.2, respectively. The load compositions were obtained from Abdel-Akher et al. [30]. The network real and reactive power losses were determined to be 199.691 kW, and 125.859 kVAr, respectively. The minimum voltage magnitude in the network increases to 0.896 p.u. at bus-54 and correspondingly the overall NVSI becomes 0.3556. In addition, the GHG emissions were determined as 5314.32 lb/h.

5.1. Assessment of EV Load Penetration Impact on Network Performance (Case 1)

In this scenario, the feeder performance was determined for different EV load penetrations and the results are listed in Table 1. It is observed that the performance of feeder is degraded as EV load penetration increases (P_d and Q_d), the real (P_{loss}) and reactive (Q_{loss}) power losses are increased, voltage profile (V_{min}) is decreased, NVSI is increased/ or stability margin is decreased. In addition, the GHG emissions increased significantly. The last column indicates the number of 100 kW rated RCSs required to meet EV load. This situation clearly indicates the need for allocation of RCSs and SPVs at optimal locations.

5.2. Optimal Allocation of RCSs for Different EV Load Penetration (Case 2)

In this scenario, the level of the negative effects of EV load penetration on the feeder performance is planned to be reduced by optimally integrating RCSs in the feeder. The predefined search space is defined by knowing the highly stable locations as per the NVSI values with $\lambda_{ev} = 1$. To determine the best locations for the RCSs, the search space is divided into three zones: bus-2 to bus-23, bus-24 to bus-56, and bus-57 to bus-85, respectively. For example, when $\lambda_{ev} = 0.1$, the required RCSs were 2. Now the search algorithm needs to find the locations of these in the above divided zones.

The best locations were bus-2, bus-24 and bus-57, respectively. The network performance for different numbers of charging ports (N_{CPs}), is presented in Table 2. Compared to Table 1, the network performance is significantly improved with the optimal location of the RCSs. The losses decreased, the voltage profile improved, the VSI increased and the GHG emissions decreased.

5.3. Optimal Allocation of RCSs and SPVs for Different EV Load Penetration (Case 3)

In this case, the performance was optimised by integrating SPVs with RCSs. The algorithm identifies the best locations for RCSs, and the best locations and sizes of the SPVs are given in Table 3. The reduced losses, improved voltage profile, increased VSI, and reduced GHG emissions are better than only the optimisation of RCSs in, as shown in Table 2. The convergence characteristics of the EPFA while solving the simultaneous optimal allocation of RCPs and SPVs are shown in Fig. 1.
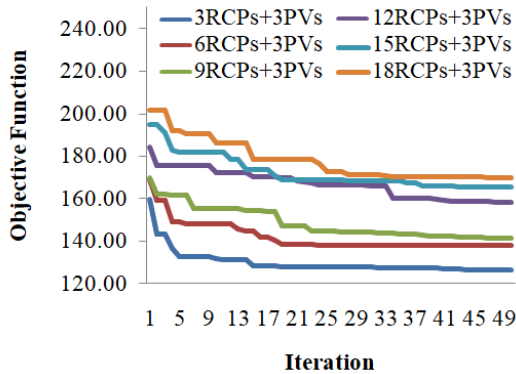
Figure 1. Convergence of EPFA for different scenarios
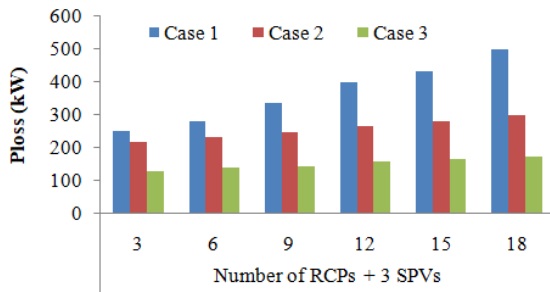
Figure 2. Comparison of P$_{loss}$
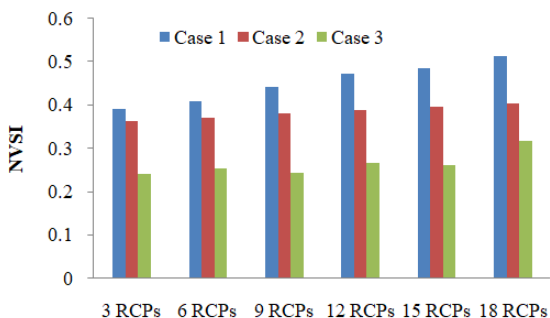
Figure 3. Comparison of NVSI
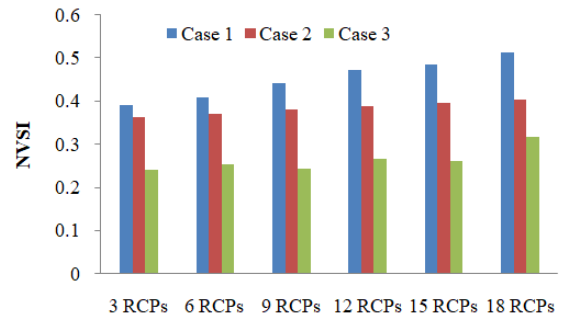
Figure 4. Comparison of GHG emissions

The three objective functions were compared individually for the three case studies. The actual power loss, NVSI, and GHG emissions are shown in Fig. 2, 3, and 4, respectively.

Fig. 2 illustrates that the losses increase notably as the EV load penetration increases in Case 1. However, in Case 2, the losses are reduced significantly by optimally placing the RCSs to accommodate the EV load. Case 3 demonstrates a further decrease in losses via simultaneous optimal allocation of reactive compensators and small-scale PV systems. This indicates an enhanced efficiency within the distribution system.

As shown in Fig. 3, the voltage stability index increased markedly with higher EV load penetration in Case 1. Case 2 results in a considerable decline by optimising the RCPs locations for a given EV load. This was further decreased in Case 3 through the joint optimal placement of reactive compensators and PV systems, demonstrating greater security.

Fig. 4 shows how GHG emissions rise prominently with the EV load rise in Case 1. However, emissions also fall in Case 3 owing to coordinated optimisation, reflecting the contribution of distributed generation to environmental benefits.

5.4. Comparative Analysis with Literature

In this case study, the proposed EPFA was used to solve the optimal allocation of SPVs on an IEEE 69-bus test system without considering EV penetration. The computational efficiency of the EPFA was compared with that of the basic PFA and AOA. In addition, the results of the EPFA were compared with those of FSA [18], TSO [19], SPPA [20], and I-GWOPSO [21].

The network initially had real and reactive power loads of 3802.10 kW and 2694.7 kVAr, respectively. With an operating voltage of 11 kV, the network initially had real and reactive power losses of approximately 225 kW and 102.17 kVAr,

respectively. The NVSI and GHG emissions were determined to be 0.4428 and 8246.13 lb/h.

The best results obtained by EPFA are as follows: locations are buses 17, 61, and 11, and the sizes in kW are 381.45, 1718.84, and 525.56,

respectively. By integrating these SPVs, the network losses decreased to 69.4285 and 34.9618 kVAr, respectively. The NVSI and GHG emissions were evaluated to be 0.8759 and 2550.419 lb/h, respectively.

Table 1. Network performance with EV load penetration

λ_{ev}	P_d (kW)	Q_d (kVAr)	P_{loss} (kW)	Q_{loss} (kVAr)	V_{min} (p.u.)	NVSI	GHG (lb/h)	N_{RCS}
0.0	2395.62	1926.84	199.691	125.859	0.8960	0.3556	5314.32	-
0.1	2594.35	1951.44	224.410	141.450	0.8894	0.3743	5771.85	2
0.2	2787.91	1974.39	250.437	157.870	0.8829	0.3923	6221.51	4
0.3	2976.99	1997.00	277.787	175.127	0.8766	0.4095	6664.68	6
0.4	3161.57	2018.78	306.342	193.147	0.8704	0.4261	7101.10	8
0.5	3341.82	2039.74	336.028	211.886	0.8643	0.4419	7530.98	9
0.6	3518.37	2060.68	366.867	231.355	0.8583	0.4573	7955.65	11
0.7	3690.67	2080.43	398.661	251.431	0.8524	0.4720	8373.56	13
0.8	3859.18	2099.55	431.409	272.113	0.8467	0.4861	8785.67	15
0.9	4024.05	2118.09	465.058	293.369	0.8410	0.4997	9192.16	16
1.0	4184.76	2135.29	499.429	315.085	0.8355	0.5127	9591.64	18

Table 2. Optimal locations of RCSs and correspondingly number of charging ports (NCPs) at each station

N_{RCS}	Bus # (N_{CPs})	P_{loss} (kW)	Q_{loss} (kVAr)	V_{min} (p.u.)	NVSI	GHG (lb/h)
3	2 (1), 24 (1), 57 (1)	214.291	135.830	0.8930	0.3642	5824.797
6	2 (2), 24 (2), 57 (2)	229.693	146.314	0.8900	0.3726	6327.947
9	2 (3), 24 (3), 57 (3)	245.944	157.339	0.8871	0.3808	6824.911
12	2 (4), 24 (4), 57 (4)	262.980	168.865	0.8842	0.3889	7315.416
15	2 (5), 24 (5), 57 (5)	280.771	180.873	0.8813	0.3968	7799.596
18	2 (6), 24 (6), 57 (6)	299.291	193.345	0.8785	0.4045	8277.580

Table 3. Optimal locations of RCSs and SPVs and correspondingly network performance

N_{RCS}	Bus # (N_{CPs})	Bus # (P_{pv})	P_{loss} (kW)	Q_{loss} (kVAr)	NVSI	GHG (lb/h)
3	2 (1), 24 (1), 57 (1)	681/26, 424/31, 252/69	126.112	78.717	0.2403	3039.629
6	2 (2), 24 (2), 57 (2)	15/78, 923/28, 547/72	137.916	85.922	0.2539	3324.331
9	2 (3), 24 (3), 57 (3)	363/55, 975/57, 272/72	141.066	88.185	0.2429	3595.688
12	2 (4), 24 (4), 57 (4)	209/57, 71/24, 1334/28	158.219	96.953	0.2667	4112.489
15	2 (5), 24 (5), 57 (5)	511/51, 650/8, 699/57	165.282	103.263	0.2617	4149.618
18	2 (6), 24 (6), 57 (6)	526/7, 1292/57, 151/24	169.793	104.790	0.3183	4380.001

Table 4. Results of SPVs allocation

Ref.	Sizes in kW/ bus #	F_1 (kW)
Base	-	225
FSA [18]	473.1/19, 591.3/11, 1859.3/61	71.02
TSO [19]	825.09/9, 405.14/22, 1650.1/61	70.25
SPPA [20]	42.8/ 57, 995/7, 102.1/6, 1768/58	98.87*
I-GWOPSO [21]	301/21, 1738/61, 508/11	68.59
AOA	379.16/18, 528.44/11. 1719.03/61	69.43
PFA	396.77/18, 1726.9/61, 463.3/66	69.69
EPFA	381.45/17, 1718.84/61, 525.56/11	69.43

* Not satisfied the constraint defined in Eq. (11).

Compared to the base case, the network performance is improved significantly in terms of reduced losses, increased stability margin, and

reduced GHG emissions. A comparison of the results with the literature and the results of other algorithms is given in Table 4. Although the results

of [20] are claimed to be better, they fail to maintain the DG limit, as given in Eq. (11), and the results are quoted here with corrections. As shown, the PFA results are better than those of the FSA [18], TSO [19], SPPA [20], and I-GWOPSO [21]. In addition, the EPFA results were better than those of PFA, and AOA was also performed competitively with EPFA.

6. Conclusion

This paper proposes concurrently optimizing the placement of rapid charging stations (RCSs) and renewable energy-based distributed generation (RE-based DG) to reduce active power losses, enhance voltage stability margins, and lower main grid greenhouse gas (GHG) emissions. An enhanced pathfinder algorithm (EPFA) inspired by the foraging, exploitation, and hunting behaviours of social animals is presented. The EPFA determines the optimal locations and sizes of RE sources and outperforms comparative global optimisation techniques owing to its superior explorative abilities. The losses and GHG emissions decreased by 69.14% and 69.07%, respectively, whereas the voltage stability margins showed a substantial increase from 0.4428 to 0.8759. Thereafter, the performance of the low-voltage feeders was assessed under increasing electric vehicle (EV) load penetration. RCSs and controllable energy storage systems are then optimised for equivalent EV loads, considerably improving the associated performance metrics. Case studies utilising IEEE 69-bus and Indian 85-bus test systems simulated diverse scenarios, demonstrating the applicability of the proposed methodology for real-time adaptation and its ability to notably enhance the low-voltage feeder function.

Although significant improvements were achieved through steady-state examination, future work could focus on considering uncertainties stemming from photovoltaic output, wind speeds, EV usage patterns, and network loading conditions. Accounting for such variability represents a key avenue for potentially strengthening results.

Nomenclature	
$P_{d,new}$	Net real power load with PV and EVs
$Q_{d,new}$	Net reactive power load with SPV and EVs
$P_{d,base}$	Base case net real and reactive power load
$Q_{d,base)}$	Base case net reactive power load
$P_{rdg(k)}$	Real power injection by SPV at bus-k, respectively
$\phi_{rdg(k)}$	Operating power factor of SPV at bus-k
$|V_{(k)}|$	Voltage magnitudes of bus-k
$|V_{(r)}|$	Voltage magnitudes of reference bus
α and β	Exponents for real and reactive power loads as per the type of load
λ_r, λ_i and λ_c	Composition factors of residential, commercial and industrial type of loads at each bus
λ_{ev}	EV load penetration in p.u.
EV_{load}	EV load in kW
$r_{(k)}$ and $x_{(k)}$	Resistance and reactance's of branch-k
$P_{d(s/s)}$	Total real power demand of the substation includes feeder load and losses
CO_2, NO_2, and SO_2	GHG emissions in lb/kWh from main grid sources
nb	Number of buses in the network

References

[1] https://ourworldindata.org/renewable-energy.

[2] https://www.iea.org/reports/global-ev-outlook-2023/trends-in-electric-light-duty-vehicles.

[3] HA, M. P., Huy, P. D., & Ramachandaramurthy, V. K. (2017). A review of the optimal allocation of distributed generation: Objectives, constraints, methods, and algorithms. Renewable and Sustainable Energy Reviews, 75, 293-312. DOI: 10.1016/j.rser.2016.10.071

[4] Ehsan, A., & Yang, Q. (2018). Optimal integration and planning of renewable distributed generation in the power distribution networks: A review of analytical techniques. Applied Energy, 210, 44-59. DOI: 10.1016/j.apenergy.2017.10.106

[5] Tolba, M. A., Rezk, H., Al-Dhaifallah, M., & Eisa, A. A. (2020). Heuristic optimization techniques for connecting renewable distributed generators on distribution grids. Neural Computing and Applications, 32, 14195-14225. DOI: 10.1007/s00521-020-04812-y

[6] Reddy, P. D. P., Reddy, V. C. V., & Manohar, T. G. (2018). Optimal renewable resources placement in distribution networks by combined power loss index and whale optimization algorithms. Journal of Electrical

Systems and Information Technology, 5(2), 175-191. DOI: 10.1016/j.jesit.2017.05.006

[7] Reddy, P. D. P., Reddy, V. C. V., & Manohar, T. G. (2018). Ant Lion optimization algorithm for optimal sizing of renewable energy resources for loss reduction in distribution systems. Journal of Electrical Systems and Information Technology, 5(3), 663-680. DOI: 10.1016/j.jesit.2017.06.001

[8] Suresh, M. C. V., & Belwin, E. J. (2018). Optimal DG placement for benefit maximization in distribution networks by using Dragonfly algorithm. Renewables: Wind, Water, and Solar, 5(1), 1-8. DOI: 10.1186/s40807-018-0050-7

[9] Reddy, P. D. P., Reddy, V. V., & Manohar, T. G. (2016). Application of flower pollination algorithm for optimal placement and sizing of distributed generation in distribution systems. Journal of Electrical Systems and Information Technology, 3(1), 14-22. DOI: 10.1016/j.jesit.2015.10.002

[10] Chithra Devi, S. A., Lakshminarasimman, L., & Balamurugan, R. (2017). Stud Krill herd Algorithm for multiple DG placement and sizing in a radial distribution system. Engineering Science and Technology, an International Journal, 20(2), 748-759. DOI: 10.1016/j.jestch.2016.11.009

[11] Ali, E. S., Abd Elazim, S. M., & Abdelaziz, A. Y. (2017). Ant Lion Optimization Algorithm for optimal location and sizing of renewable distributed generations. Renewable Energy, 101, 1311-1324. DOI: 10.1016/j.renene.2016.09.023

[12] Optimal allocation of distributed generators DG based Manta Ray Foraging Optimization algorithm (MRFO). (2021). Ain Shams Engineering Journal, 12(1), 609–619. DOI: 10.1016/j.asej.2020.07.009

[13] Optimal placement and sizing of multiple distributed generating units in distribution networks by invasive weed optimization algorithm. (2016). Ain Shams Engineering Journal, 7(2), 683–694. DOI: 10.1016/j.asej.2015.05.014

[14] Hemeida, M. G., Alkhalaf, S., Senjyu, T., Ibrahim, A., Ahmed, M., & Bahaa-Eldin, A. M. (2021). Optimal probabilistic location of DGs using Monte Carlo simulation based different bio-inspired algorithms. Ain Shams Engineering Journal, 12(3), 2735-2762. DOI: 10.1016/j.asej.2021.02.007

[15] Ali, M. H., Kamel, S., Hassan, M. H., Tostado-Véliz, M., & Zawbaa, H. M. (2022). An improved wild horse optimization algorithm for reliability based optimal DG planning of radial distribution networks. Energy Reports, 8, 582-604. DOI: 10.1016/j.egyr.2021.12.023

[16] Janamala, V., & Radha Rani, K. (2022). Optimal allocation of solar photovoltaic distributed generation in electrical distribution networks using Archimedes optimization algorithm. Clean Energy, 6(2), 271-287. DOI: 10.1093/ce/zkac010

[17] Selim, A., Kamel, S., Alghamdi, A. S., & Jurado, F. (2020). Optimal placement of DGs in distribution system using an improved harris hawks optimizer based on single-and multi-objective approaches. IEEE Access, 8, 52815-52829. 10.1109/access.2020.2980245

[18] Janamala, V., Kamal Kumar, U., & Pandraju, T. K. S. (2021). Future search algorithm for optimal integration of distributed generation and electric vehicle fleets in radial distribution networks considering techno-environmental aspects. SN Applied Sciences, 3(4), 464. DOI: 10.1007/s42452-021-04466-y

[19] Bhadoriya, J. S., & Gupta, A. R. (2021). A novel transient search optimization for optimal allocation of multiple distributed generator in the radial electrical distribution network. International Journal of Emerging Electric Power Systems, 23(1), 23-45. DOI: 10.1515/ijeeps-2021-0001

[20] Shahzad, M., Akram, W., Arif, M., Khan, U., & Ullah, B. (2021). Optimal siting and sizing of distributed generators by strawberry plant propagation algorithm. Energies, 14(6), 1744. DOI: 10.3390/en14061744

[21] Akbar, M. I., Kazmi, S. A. A., Alrumayh, O., Khan, Z. A., Altamimi, A., & Malik, M. M. (2022). A novel hybrid optimization-based algorithm for the single and multi-objective achievement with optimal DG allocations in distribution networks. IEEE Access, 10, 25669-25687. DOI: 10.1109/access.2022.3155484

[22] Das, H. S., Rahman, M. M., Li, S., & Tan, C. W. (2020). Electric vehicles standards, charging infrastructure, and impact on grid integration: A technological review. Renewable and Sustainable Energy Reviews, 120, 109618. 10.1016/j.rser.2019.109618

[23] Zeb, M. Z., Imran, K., Khattak, A., Janjua, A. K., Pal, A., Nadeem, M., ... & Khan, S. (2020). Optimal placement of electric vehicle charging

stations in the active distribution network. IEEE Access, 8, 68124-68134. DOI: 10.1109/access.2020.2984127

[24] Khan, W., Ahmad, F., & Alam, M. S. (2019). Fast EV charging station integration with grid ensuring optimal and quality power exchange. Engineering Science and Technology, an International Journal, 22(1), 143-152. DOI: 10.1016/j.jestch.2018.08.005

[25] Dai, Q., Liu, J., & Wei, Q. (2019). Optimal photovoltaic/battery energy storage/electric vehicle charging station design based on multi-agent particle swarm optimization algorithm. Sustainability, 11(7), 1973. DOI: 10.3390/su11071973

[26] Injeti, S. K., & Thunuguntla, V. K. (2020). Optimal integration of DGs into radial distribution network in the presence of plug-in electric vehicles to minimize daily active power losses and to improve the voltage profile of the system using bio-inspired optimization algorithms. Protection and Control of Modern Power Systems, 5, 1-15. DOI: 10.1186/s41601-019-0149-xA new meta-heuristic optimizer: Pathfinder algorithm. (2019). Applied Soft Computing, 78, 545–568. DOI: 10.1016/j.asoc.2019.03.012

[27] An enhanced pathfinder algorithm for engineering optimization problems. (2021). Engineering with Computers, 38(S2), 1481–1503. DOI: 10.1007/s00366-021-01286-x

[28] A new power flow method for radial distribution systems including voltage dependent load models. (2005). Electric Power Systems Research, 76(1-3), 106–114. DOI: 10.1016/j.epsr.2005.05.008

[29] Abdel-Akher, M., Eid, A., & Ali, A. (2017). Effective demand side scheme for PHEVs operation considering voltage stability of power distribution systems. International Journal of Emerging Electric Power Systems, 18(2), 20160041. DOI: 10.1515/ijeeps-2016-0041

[30] Janamala, V., & Radha Rani, K. (2022). Optimal allocation of solar photovoltaic distributed generation in electrical distribution networks using Archimedes optimization algorithm. Clean Energy, 6(2), 271-287.

[31] Rani, K. R., Rani, P. S., Chaitanya, N., & Janamala, V. (2022). Improved Bald Eagle Search for Optimal Allocation of D-STATCOM in Modern Electrical Distribution Networks with Emerging Loads. International Journal of Intelligent Engineering & Systems, 15(2), 554-563. DOI: 10.22266/ijies2022.0430.49